Jpn. J. Appl. Phys. Vol. 42 (2003) pp. 6731–6736
Part 1, No. 11, November 2003

Photomodulated Second-Harmonic Generation at Silicon-Silicon Oxide Interfaces: From Modeling to Application

Elena D. MISHINA[1,2*], Nobuko TANIMURA[2], Seiichiro NAKABAYASHI[2], Oleg A. AKTSIPETROV[3] and Michael C. DOWNER[4]

[1]*Moscow Institute of Radioengineering, Electronics and Automation, prosp. Vernadskogo 78, Moscow 117454, Russia*
[2]*Department of Chemistry, Faculty of Science, Saitama University, Saitama 338-8570, Japan*
[3]*Physics Department, Moscow State University, Moscow 117899, Russia*
[4]*Texas Material Institute, University of Texas, Austin, Texas 78712-1081, USA*

(Received December 11, 2002; revised May 1, 2003; accepted July 8, 2003; published November 10, 2003)

A photomodulation technique based on the nonlinear-optical process of second-harmonic generation (SHG) is developed for characterizing Si/SiO_2 interfaces and silicon-based metal-oxide-semiconductor (MOS) structures. The mechanisms of photoinduced SHG are discussed and a quantitative model of the SHG response is formulated. A method of extracting parameters of the Si/SiO_2 interface from *in situ*-photomodulated-SHG measurements is proposed. The accuracy of the technique for measuring parameters of silicon-based MOS structures is estimated. [DOI: 10.1143/JJAP.42.6731]

KEYWORDS: MOS structure, photomodulation, nonlinear optics

1. Introduction

Because the Si/SiO_2 system forms the basis of modern microelectronics, techniques for characterizing it are well developed on the industrial level. Traditionally, the industry has relied most heavily on electrical measurements performed *ex situ* on fully fabricated Si/SiO_2-based devices (or their prototypes). Recently, noncontact optical and X-ray (including synchrotron radiation) techniques that allow *in situ* control at early stages of fabrication have been gaining importance. Photoreflectance spectroscopy is used for measuring the surface potential[1,2] and interface stress.[3] Fourier transform IR reflection spectroscopy is used for the study of interface stress.[4] Spectroscopic ellipsometry is used for measuring the oxide thickness and its spatial distribution.[5] Optical techniques are particularly useful because they enable control of the uniformity of interface parameters in current industry-standard 30 cm silicon wafers.

Optical second-harmonic generation (SHG) provides a particularly sensitive tool for characterizing buried interfaces, such as the technologically important $Si–SiO_2$ interface (see ref. 6 for a review). Two aspects of SHG techniques deserve emphasis. First, like other optical techniques, SHG can be adapted readily to a variety of processing environments, and is useful both before and after device fabrication. Second, numerous interface properties usually influence the SHG signal and can therefore (in principle) be measured. These include atomic-scale roughness,[7,8] crystalline symmetry,[9] doping type and concentration,[10] interface charge[6,11] and strain.[12] In addition, when a dc electric field is applied across the Si/SiO_2 interface, an electric-field-induced SH (EFISH) signal arises that is sensitive to the properties of the space-charge region. EFISH exists not only when an external voltage is applied (as in a MOS structure), but also at the bare $Si–SiO_2$ interface, because of initial band bending.[13] Complete theoretical modeling and calculations of EFISH generation and its relation to parameters of Si/SiO_2 systems were presented in ref. 14. However, practical application of EFISH generation to quantitative characterization of Si/SiO_2 space-charge regions requires the development of refined techniques that isolate EFISH from competing contributions to the overall SHG signal. Modulation SHG techniques enable this isolation. Because of their derivative nature,[15] modulation techniques sharpen characteristic spectral features of the sample that are related to the modulated quantity. As an example, electromodulation (often called electroreflectance in optical studies), in which an external electric field is modulated, has previously been combined with SHG, but its application was restricted to characterizing fully fabricated MOS structures.[14] On the other hand, photo-modulation, in which the space-charge regions (and possibly other surface properties) are modulated by a chopped pump laser and probed by a second beam of lower power density, can be applied both to fabricated devices and bare $Si–SiO_2$ systems. Vardeny *et al.*[16] developed the linear photomodulation technique, so called because the probe beam measures the modulated *linear* optical properties of the sample.

In this paper, we demonstrate a *nonlinear* photomodulation technique, in which the probe laser beam measures SHG intensity from a region of the sample surface that is modulated by a chopped pump laser beam. This technique allows us to isolate the EFISH contribution of interest, thereby allowing a direct measurement of flat-band voltage and related electrical properties of Si/SiO_2 systems. We also develop a method of extracting the parameters of the Si/SiO_2 interface from the characteristics of *in situ*-photomodulated SHG. In the next section, we use the results of calculations in ref. 14 to develop a model of photomodulated EFISH generation.

2. Model Calculation

The SH field generated at a biased Si/SiO_2 interface consists of two parts, one independent of, and the other dependent on, the DC field ($E^0_{2\omega}$ and $E^{DC}_{2\omega}$, respectively). The former is a superposition of a bulk quadrupole field $E^{0,BQ}_{2\omega}$, generated throughout the absorption depth, and an interface dipole field $E^{0,SD}_{2\omega}$ generated locally at the Si/SiO_2 interface. The latter is generated in the space-charge region (SCR) of the semiconductor. Thus, the total SHG intensity at the Si/SiO_2-based MOS structure can be written as

*E-mail address: elena_mish@yahoo.com

$$I_{2\omega} = (E_{2\omega}^{0,\mathrm{SD}} + E_{2\omega}^{0,\mathrm{BQ}} + E_{2\omega}^{\mathrm{DC}})^2. \quad (1)$$

Since the relative magnitude of the three contributions in eq. (1) depends on doping concentration, preparation condition and probing wavelength, it is not in general possible to neglect any one of them. Moreover, the fields are complex. The electric-field-induced component can be found by integrating the product of a DC field $E_0(z)$ and the wave propagation factor over the SCR as

$$E_{2\omega}^{\mathrm{DC}} \propto \chi_{\mathrm{eff}}^{(3),\mathrm{BD}} \int_0^{+\infty} E_0(z) \exp(i\Delta z) dz, \quad (2)$$

where $\chi_{\mathrm{eff}}^{(3),\mathrm{BD}}$ is the third-order bulk-dipole nonlinear susceptibility (which, unlike its second-order counterpart, is non-zero in centrosymmetric media), the z-axis is normal to the surface, and $\Delta = (k_{2\omega,z} + 2k_{\omega,z})$, with $k_{\omega,z}$ and $k_{2\omega,z}$ the z-components of the fundamental and SH wave vectors.

The spatial distribution of $E_0(z)$ across the silicon SCR is calculated by solving the first integral of the Poisson equation, yielding, within the Boltzmann approximation, the well-known expression,[17)]

$$\begin{aligned} E_0^2(z) &= \frac{8\pi k p_0}{\varepsilon_{\mathrm{sc}}} \left((e^{-\beta\varphi(z)} + \beta\varphi(z) - 1) \right. \\ &\quad \left. + \frac{n_0}{p_0} (e^{\beta\varphi(z)} - \beta\varphi(z) - 1) \right) \\ &= \frac{8\pi k p_0}{\varepsilon_{\mathrm{sc}}} F^2\left(\beta\varphi(z), \frac{n_0}{p_0}\right), \end{aligned} \quad (3)$$

where $p_0 = N_{\mathrm{A}}$, $n_0 = N_{\mathrm{i}}^2/N_{\mathrm{A}}$, N_{i} and N_{A} are respectively intrinsic carrier and doping concentrations (donor for p-type semiconductor), k is the Boltzmann constant, $\varepsilon_{\mathrm{sc}}$ is the static dielectric constant of silicon, $\beta = e/kT$, e is the electron charge, T is the temperature, and $\varphi(z)$ is the potential within the SCR. Hereafter, all equations are written for a p-type semiconductor. For n-type semiconductors, the polarity of the voltage should be reversed.

For an illuminated surface, a quasi-Fermi-level approximation can be used that gives a modified expression for the DC electric field inside the SCR as[18)]

$$\begin{aligned} E_0^{*2}(z) &= \frac{8\pi k p_0}{\varepsilon_{\mathrm{sc}}} \left(F^2\left(\beta\varphi^*(z), \frac{n_0}{p_0}\right) \right. \\ &\quad \left. + \frac{n_0}{p_0} \Delta_n (e^{-\beta\varphi^*(z)} + e^{\beta\varphi^*(z)} - 2) \right), \end{aligned} \quad (4)$$

where $\Delta_n = \partial n/n_0$ and ∂n is the minority carrier excess due to illumination. The carrier excess is inhomogeneous and can be written, following ref. 19, as $\partial n(z) = \alpha J \exp(-\alpha z)$, where J is the effective photon flux (equal to the incident photon flux multiplied by the surface optical transmission and the sample quantum efficiency) and α is the absorption coefficient.

For samples illuminated with a conventional femtosecond oscillator, the pulse repetition rate is about 80 MHz (corresponding to a 13 ns interval between pulses) and the excitation time is about 100 fs, whereas the time scale for carrier recombination is 3 µs. It was first shown in ref. 11 that, with such illumination, cumulative pulse-to-pulse effects determine the carrier excess δn in the SCR, and eq. (4) should be used for the steady state. The photoinduced density of carriers saturates in approximately 10 µs. Therefore with a recording time of 1 s, the saturation value should be considered for the carrier excess.

From eqs. (1)–(3) SHG intensity can be related to the interface potential $\varphi_{\mathrm{int}} = \varphi(z = 0)$. In order to relate SHG intensity to the total voltage drop U across the MOS structure (a measured quantity), we use the boundary conditions at the Si/SiO_2 interface. These give

$$U = (\varepsilon_{\mathrm{sc}} E_{\mathrm{int}}^{\mathrm{DC}}(\varphi_{\mathrm{int}}) - 4\pi Q) - \frac{L_{\mathrm{ox}}}{\varepsilon_{\mathrm{ox}}} + \varphi_{\mathrm{int}}, \quad (5)$$

where $E_{\mathrm{int}}^{\mathrm{DC}}$ is the interface DC field, $\varepsilon_{\mathrm{ox}}$ and L_{ox} are the dielectric constant and thickness of the oxide layer, respectively, and Q is the interface charge (which includes chargeable interface traps as well as charge localized in the oxide layer). Using eqs. (1)–(5), we relate SHG intensity to applied voltage in a parametric form. This relationship includes the following basic parameters of the MOS structure: doping concentration (and carrier excess in case of illumination), oxide thickness, interface and oxide charge. Additionally, it includes the SHG field-independent term $E_{2\omega}^0 = E_{2\omega}^{0,\mathrm{SD}} + E_{2\omega}^{0,\mathrm{BQ}}$.

The presence of this last term in the SHG field prevents a direct measurement of the interface potential (and other related parameters such as flat-band potential and interface charge) because the minimum of the SHG intensity-voltage dependence is shifted from the flat-band voltage by a value that depends on the ratio $E_{2\omega}^0/E_{2\omega}^{\mathrm{DC}}$. Thus $E_{2\omega}^0$ must be extracted by fitting the SHG intensity–voltage dependence, using a numerical solution of the Poisson equation and numerical integration of eq. (2). This highly indirect procedure compromises the reliability of the SHG probe. Photomodulated SHG helps to solve this problem. Specifically, flat band voltage U_{fb} is easily identified as the voltage U at which the SHG intensity vs U curve *with* illumination (hereafter the "light" or "on" curve $I_{2\omega}^{\mathrm{light}}(U)$) crosses the corresponding curve *without* illumination (hereafter the "dark" or "off" curve $I_{2\omega}^{\mathrm{dark}}(U)$). Since $E_{2\omega}^{\mathrm{DC}} = 0$ at this point, SHG intensity at this voltage immediately yields $E_{2\omega}^0$. We define SHG photomodulation efficiency $\eta(U) = \Delta I_{2\omega}/I_{2\omega} = (I_{2\omega}^{\mathrm{off}} - I_{2\omega}^{\mathrm{on}})/I_{2\omega}^{\mathrm{off}}$, analogously to linear photomodulation. Thus $\eta = 0$ for $U = U_{\mathrm{fb}}$.

Figure 1 shows examples of calculations based on the model presented above. Two types of silicon-based MOS structures are considered: highly doped ($N_{\mathrm{A}} = 10^{18}\,\mathrm{cm}^{-3}$, left panels) and mediumdoped ($N_{\mathrm{A}} = 10^{16}\,\mathrm{cm}^{-3}$, right panels). The carrier excesses for both structures correspond to approximately the same illumination power densities. The difference in of Δ_n originates from the difference in the initial concentrations of minority carriers. Figures 1(a) and 1(b) show the real and imaginary parts of the SHG field without ($\Delta_n = 0$) and with illumination ($\Delta_n \neq 0$). For both structures, illumination changes the real part of the SHG field more than the imaginary part. This can be understood by considering the spatial distribution of the integrand of eq. (2) [Figs. 1(c) and 1(d)]. Illumination preferentially modulates the DC field $E_0(z)$ in the immediate subsurface region (i.e., near $z = 0$), with a fast decay inside the SCR (screening effect[20)]). Thus the product of $E_0(z)$ and the real ($\cos \Delta z$) part

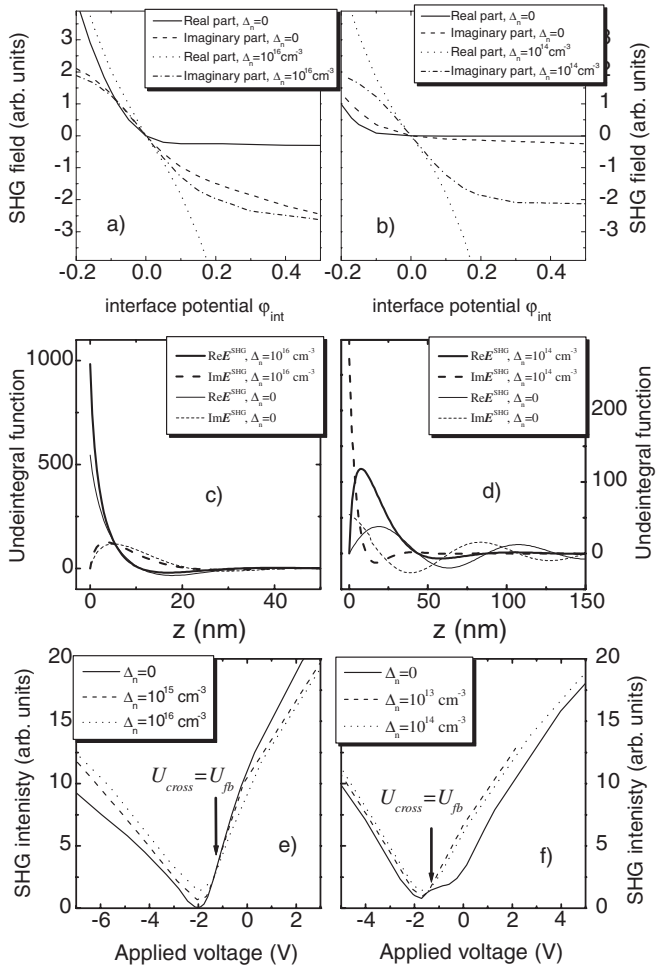

Fig. 1. Calculations of photomodulated SHG intensity for highly doped ($N_A = 10^{18}$ cm^{-3}, left panels) and medium-doped ($N_A = 10^{16}$ cm^{-3}, right panels) silicon. Panels (a) and (b) show real and imaginary parts of the SHG field as a function of interface potential with (carrier excess $\Delta_n \neq 0$) and without ($\Delta_n = 0$) illumination; panels (c) and (d) show spatial distribution of the real and imaginary parts of the integrand of eq. (2); panels (e) and (f) show SHG intensity as function of external voltage; oxide state density $N_{ox} = 2 \times 10^{12}$ cm^{-2}. Arrows indicate cross points corresponding to flat-band voltage U_{fb}.

of the propagation factor changes more strongly than the product of $E_0(z)$ and the imaginary ($\sin \Delta z$) part. In addition to the surface value, the whole spatial distribution of the integrand changes as well, giving rise to a change in SHG intensity. For highly doped Si, "light" and "dark" SHG curves cross each other at a single point [Fig. 1(e)]. For lightly doped Si they may touch or cross twice [Fig. 1(f)]. In the latter case, the crossing voltage of smaller absolute value is U_{fb}.

The spatial distribution of the integrand shows the possibility for depth profiling within the SCR, because often the probing depth of SHG is comparable to the SCR depth. In fact for ultraviolet SH wavelengths, the former is often smaller because strong adsorption limits escape depth of SH light to 100–200 Å. In either case, illumination of the Si/SiO_2 interface changes the actual effective thickness within which the SHG wave is generated. Thus by changing the illumination power, the probing depth can be modified.

3. Experiment

For the SH photomodulation experiments, the output of a 120 fs unamplified Ti-sapphire laser tunable from 710 to 800 nm was used. The fundamental beam was split into two parts: the SH generating probe with an average power of 10–20 mW and a pump with an average power of up to 300 mW. The *p*-polarized probe beam was focused onto the sample at a 45° angle of incidence with a spot diameter of approximately 50 µm. The reflected *p*-polarized SHG signal was selected by a polarization analyzer and color filters and directed into a photomultiplier tube and photon-counting system. The pump beam was modulated by a mechanical chopper and focused at normal incidence to a spot of approximately 200 µm diameter. The frequency of the chopper could be varied over the range of 100–4000 Hz. A small split-off portion of the fundamental beam was focused through a *z*-cut quartz crystal that provided a reference SHG signal. SHG intensities with ("light") and without ("dark") pump illumination were measured by the photon-counting system working in a gate mode. A computer then calculated the photomodulation efficiency η as experimental parameters varied.

MOS structures were fabricated from two types of Si(001) wafers: (I)-a highly doped *n*-type (0.05 Ωcm, Sb doped) wafer covered by a 19-nm-thick SiO_2 film, and (II)-a lightly doped *p*-type (15 Ωcm, B doped) wafer with a 8.7-nm-thick SiO_2 film. A 3 nm semitransparent chromium cap layer, and an ohmic aluminum backside electrode were evaporated onto the samples. External bias was applied between the chromium and aluminum electrodes. The SHG response from the chromium layer was verified to be negligible in comparison with the SHG signal from the buried Si(001)–SiO_2 interface. Capacitance-voltage dependences were measured using an impedance analyzer in the frequency range of 0.1–50 kHz. In the Mott-Schottky plot $C^{-2}(U)$ the voltage where the line of linear extrapolation intersects the voltage axes yields the value of U_{fb}.[21]

4. Results and Discussion

4.1 Voltage dependence of the SHG intensity

Figure 2 shows the experimental dependences of the SHG intensity on the applied voltage in the "dark" and "light" phases. For the highly doped Si/SiO_2-MOS structure [Fig. 2(a)] the "light" curve is shifted left and upward from the "dark" curve. A single cross point is observed at $U_{cross} = -1.8 \pm 0.1$ V, in good agreement with the Mott–Shottky plot [Fig. 2(a), inset] which gives $U_{fb} = -1.7 \pm 0.1$ V. The cross point is shifted significantly (approximately 1 V) from the minimum of the intensity–voltage dependence, as discussed in §2.

For the lightly doped structure [Fig. 2(b)] the difference between the "dark" and "light" dependences is smaller. The cross point of the two curves is shifted from the minimum by 0.25 V, and occurs at $U_{cross} = -1.75 \pm 0.15$ V, again in good agreement with the Mott–Shottky plot [Fig. 2(b), inset] which gives $U_{fb} = -1.6 \pm 0.1$ V. A deviation from a smooth quasi-parabolic behavior is observed in agreement with the calculated dependences (see circular inset for details). Thin lines are results of model calculations with the parameters of the real MOS structure.

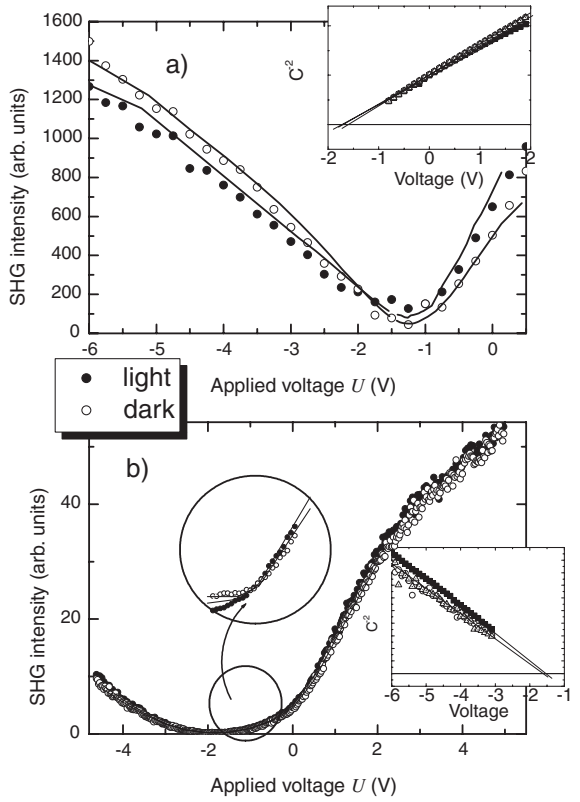

Fig. 2. Voltage dependences of photomodulated SHG intensity in "dark" (open circles) and "light" (filled circles) phases; (a) n-Si, 0.01 Ωcm, $d_{ox} = 19$ nm; (b) p-Si, 15 Ωcm, $d_{ox} = 10$ nm (circular inset shows a zoomed view of the potential range −2–−1.5 V). Excitation and probing wavelength is 732 nm, pump power 100 mW. Thin lines are model calculations with the parameters of the real MOS structure, and $N_{ox} = 1.3 \times 10^{12}\,cm^{-2}$, $\Delta_n = 8 \times 10^{15}\,cm^{-3}$ for (a) and $N_{ox} = 2 \times 10^{12}\,cm^{-2}$, $\Delta_n = 5 \times 10^{12}\,cm^{-3}$ for (b). Rectangular insets: dependences of the reversed square capacitance on the applied voltage (Mott–Schottky plot) measured at different frequencies (□—1 kHz, ○—5 kHz, and △—10 kHz).

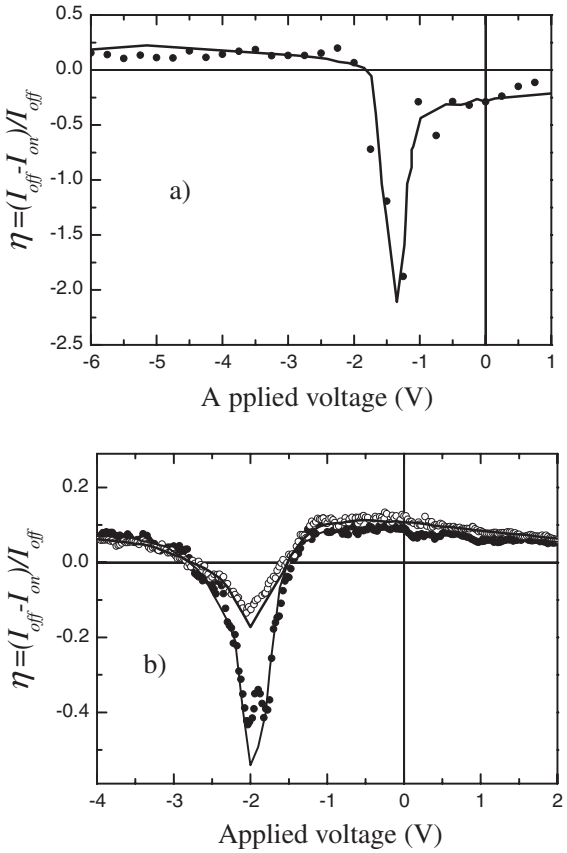

Fig. 3. The voltage dependence of the efficiency of the SHG photomodulation: (a) n-Si, average illuminating power 100 mW; (b) p-Si, average illuminating power 100 mW (filled circles) and 60 mW (open circles) Lines: model calculations. Experimental and model parameters are the same as in Fig. 2.

For both structures, optical data agree within the error bar with the results of conventional electrical data, thus validating the interpretation of the cross point of the "light" and "dark" curves as the flat band voltage: $U_{cross} = U_{fb}$.

Figures 3(a) and 3(b) show the dependence of the photomodulation efficiency η on applied voltage for highly and lightly doped silicon structures, respectively. A sharp minimum (maximum absolute value) corresponding to the minimum of $I_{2\omega}(U)$ in the dark phase is evident. Figure 3(b) shows $\eta(U)$ at low (open circles) and high (filled circles) pump powers. The magnitude of $\eta(U)$ increases with illumination power, but the position of the cross point does not change. The thin lines in Fig. 3 are a result of calculations of $\eta(U)$ using the experimental sample and illumination parameters. The value of the field-independent term was taken as the square root of the SHG intensity at the cross point.

The experimental data agree well with the model. Our model calculations assumed, as is standard in modeling photoreflection,[17] that the pump modulates SHG solely by generating electron-hole pairs in the SCR. We caution that femtosecond pump pulses of higher fluence than those used here can also change SHG by irreversibly charging the oxide via internal photoemission of electrons from Si to SiO_2.[14] The latter effect is cumulative, builds up over 60 s and becomes stronger with thinner oxides. We avoided such surface charging in our experiments by using relatively low pump power (order of magnitude lower than that in ref. 14) and relatively thick oxides (>9 nm). If this effect were present in our experiments, the cross point (flat-band voltage) would have shifted with changing laser fluence and the voltage dependence of the SHG intensity would become irreversible. Neither effect was observed.

4.2 Spectral dependence of the SHG intensity

In linear photoreflectance, analysis of the semiconductor surface is based on Franz–Keldysh oscillations which allow the band gap of the semiconductor and the interface states spectrum to be calculated (for silicon, see ref. 3). Compared with unmodulated linear reflectance, the structure of the photomodulated spectrum is much sharper, since the latter is described by the third derivative of the reflectivity. In the linear reflectivity, only E_1 and E_0 resonances are well resolved within the spectral range of 2–4 eV, without any fine structure.

Figure 4(a) shows unmodulated SHG spectra of our p-doped MOS structure. For bias $U = +3$ V (filled circles), the spectrum is similar to the linear reflection spectrum, with a broad E_1 resonance at 3.4 eV. For flat-band bias (open circles), this feature is slightly redshifted. This difference results from a change with bias of the relative importance of

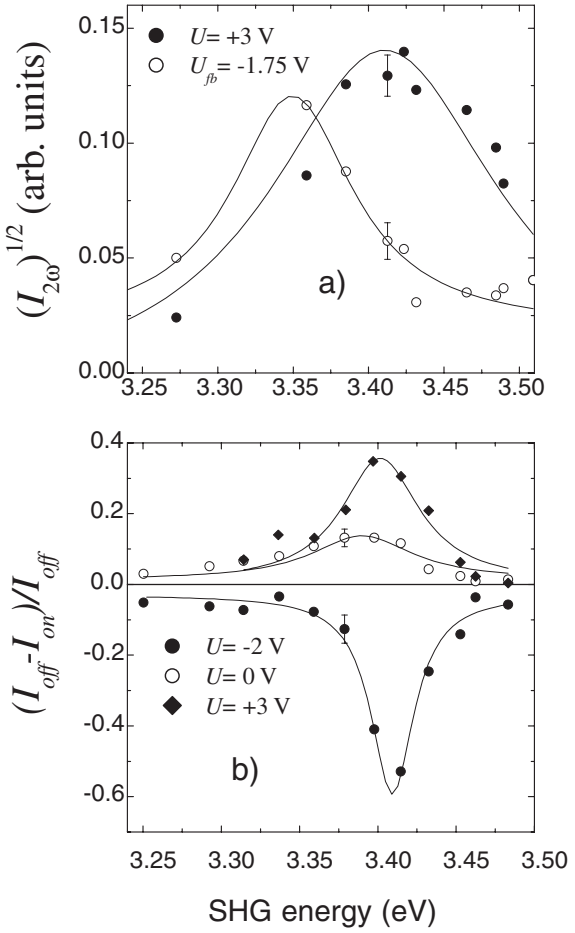

Fig. 4. Spectral dependence of the SHG intensity (a) and photomodulation efficiency (b) in p-Si MOS structure measured at different voltages. Lines—guide to eye.

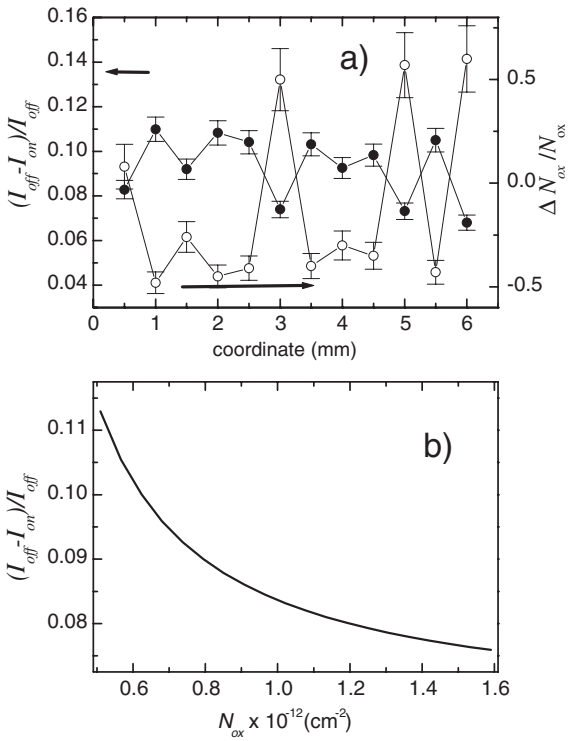

Fig. 5. (a) For different positions of the laser spot on unbiased n-Si sample ($U = 0$) experimental SHG photomodulation efficiency (filled circles, left scale) and calculated N_{ox} (open circles, right scale). (b) Calibration of photomodulated SHG intensity vs the oxide trap density for n-type MOS structure (external voltage $U = 0$) with the use of $\eta(U)$ dependence plotted in Fig. 3(a).

the three contributions in eq. (1), as discussed further below and elsewhere.[10,12] For comparison, we measured the photomodulated spectra of the same Si/SiO_2 MOS structure in the range of 3.2–3.5 eV [see Fig. 4(b)]. The bulk resonance at 3.4 eV was observed with a sharper peak than for unmodulated SHG. These measurements show that maximum SHG photomodulation efficiency is achieved with a resonance wavelength of 732 nm (SHG photon energy 3.42 eV) for the fundamental wave. No fine structure was observed in the portion of the photomodulated SHG spectrum measured [see Fig. 4(b)].

For the flat-band voltage, the bulk electric dipole contribution $E_{2\omega}^{DC}$ equals zero. Bulk quadrupole $E_{2\omega}^{0,BQ}$ and surface dipole $E_{2\omega}^{0,SD}$ contributions in this case can be observed without interference with the bulk electric dipole contribution. Figure 4(a) (open circles) shows the SHG spectrum measured for the flat-band voltage. Filled circles in the same panel show the spectrum measured at a positive voltage. These spectra reveal maxima at 3.35 and 3.43 eV, respectively. The latter is consistent with the E_1 resonance of bulk Si, as expected for the bulk-dominated EFISH spectrum. The redshift in the former spectrum reflects unique interfacial properties. For oxidized silicon, the interface stress is most probably the reason for the redshift of the E_1 peak. This opens the way for measuring the surface dipole contribution and properties of the surface related to this contribution. The stress resulting from the mismatching of the lattice constants of silicon and silicon oxide may reach several kbar[22] or in other words approximately 1% of a volume change.[23]

4.3 Measurements of Si/SiO_2 system parameters

Based on the developed technique, we show an example of the mapping of the Si/SiO_2 structure. For *qualitative* characterization, we scanned the laser beam along the silicon surface while measuring the photomodulation efficiency. The distribution of the modulation efficiency around the average value [see Fig. 5(a), left scale] reflects the distribution of the MOS structure parameters. The main advantage of such mapping is that inhomogeneity of the surface states can be obtained directly on a silicon wafer during an intermediate stage of MOS structure fabrication, prior to the gate electrode deposition.

For *quantitative* characterization, the SHG photomodulation efficiency must be calibrated against density of interface states. This can be carried out only on a test MOS structure subjected to the same treatment as the monitored silicon wafer. For this MOS structure, the complete procedure described in the previous section should be implemented to obtain the ratio between photomodulation efficiency and applied voltage [as in Fig. 3(a)]. This calibration curve can be used for characterizing the Si/SiO_2 interface of the same doping and oxide thickness. Then the photomodulation efficiency as a function of the density of the interface states should be *calculated* using the described model [Fig. 5(b)]. The map can then be transferred to the N_{ox} units [Fig. 5(a), right scale, where $\Delta N_{ox}/N_{ox}$ is the relative deviation of the

density of the interface states from its average value].

The sensitivity of the suggested technique for measuring the absolute values of the interface states density is determined by the accuracy of the calibration, which, in turn, is determined by fitting of the SHG intensity/voltage dependence. Spatial resolution of these measurements is determined by the probe laser spot, which is 50 μm in our experiments, but can be reduced to 1 μm.

For the flat-band condition, the value of the surface SHG field can be measured which indicates qualitatively the value of the interface stress. However for quantitative measurement of the interface stress, the microscopic modeling of the nonlinear optical response for the strained interface should be developed analogously to linear photoreflectance.[3)]

5. Conclusions

We have developed a noncontact photomodulation technique based on optical SHG and demonstrated its usefulness for characterizing the electrical properties of the $Si–SiO_2$ interface and the underlying SCR. The technique is equally applicable to MOS devices and to unprocessed wafers. We have demonstrated direct, accurate measurement of the flat-band potential in good agreement with standard electrical data, as well as quantitative probing of potential, charge and density of states at the Si/SiO_2 interface both at a fixed position and as a function of position on the wafer. Variations of photomodulation efficiency with applied bias and illumination intensity have been measured, quantitatively modeled and related to $Si–SiO_2$ system parameters. The presence of sharper features in photomodulated SHG spectra than in unmodulated spectra has been demonstrated. There are no technical restrictions for improving the technique to enable measurement of variations in interface defect density across a wafer with $\sim$1 μm spatial resolution, and of the depth profile of the SCR.

Aknowledgments

This work is supported by the Research for the Future (RFTF) Program and by the Japanese Society for the Promotion of Science. Experimental work at U. Texas was supported by the Robert Welch Foundation (Grant F-1038) and the U.S. National Science Foundation (Grants DMR-0207295 and PHY-0114336).

1) D. E. Aspnes: Surf. Sci. **37** (1973) 418.
2) M. Agata, H. Eada, O. Maida, K. Eriguchi, A. Fujimoto, T. Kanashima and M. Okuyama: Jpn. J. Appl. Phys. **39** (2000) 2040.
3) M. Sohgawa, M. Agata, T. Kanashima, K. Yamashita, K. Eriguchi, A. Fujimoto and M. Okuyama: Jpn. J. Appl. Phys. **40** (2001) 2844.
4) Y. Jia, Y. Liang, Yi. Liu, Yu. Liu and D. Shen: Thin Solid Films **370** (2000) 199.
5) A. H. Jajatissa, T. Yamaguchi, M. Nasu and M. Aoyama: Jpn. J. Appl. Phys. **36** (1997) 2581.
6) G. Lüpke: Surf. Sci. Report **35** (1999) 75.
7) O. A. Aktsipetrov, I. M. Baranova and Yu. A. Il'inskii: Sov. Phys. JETP **64** (1986) 167.
8) J. I. Dadap, B. Doris, Q. Deng, M. C. Downer, J. K. Lowell and A. C. Diebold: Appl. Phys. Lett. **64** (1994) 2139.
9) G. Lüpke, D. J. Bottomley and H. M. van Driel: Phys. Rev. B **47** (1993) 10389.
10) D. Lim, M. C. Downer and J. G. Ekerdt: Appl. Phys. Lett. **77** (2000) 181.
11) J. G. Mihaychuk, N. Shamir and H. M. van Driel: Phys. Rev. B **59** (1999) 2164.
12) W. Daum, H.-J. Krause, U. Reichel and H. Ibah: Phys. Rev. Lett. **71** (1993) 1234.
13) J. I. Dadap, Z. Xu, X. F. Hu, M. C. Downer, N. M. Russelt, J. G. Ekerdt and O. A. Aktsipetrov: Phys. Rev. B **56** (1997) 13367.
14) O. A. Aktsipetrov, A. A. Fedyanin, A. V. Melnikov, E. D. Mishina, A. N. Rubtsov, M. H. Anderson, P. T. Wilson, M. ter Beek, X. F. Hu, J. I. Dadap and M. C. Downer: Phys. Rev. B **60** (1999) 8924.
15) M. Cardona: *Modulation spectroscopy* (Academic Press, NY, 1969).
16) Z. Vardeny, J. Strait, D. Pfost, J. Tauc and B. Abeles: Phys. Rev. Lett. **48** (1982) 1132.
17) M. Sze: *Physics of Semiconductor Devices* (Wiley, New York, 1981) Chap. 7.
18) L. Kronik and Y. Shapira: Surf. Sci. Reports **37** (1999) 1.
19) H. Lüth: *Surfaces and Interfaces of Solids* (Springer, Berlin, 1993) 2nd ed.
20) J. I. Dadap, P. T. Wilson, M. H. Anderson, M. C. Downer and M. ter Beek: Opt. Lett. **22** (1997) 901.
21) A. Barad and L. Faulkner: *Electrochemical Methods* (Wiley, NY, 1980) p. 636.
22) S. Logothetidis and S. Boultadakis: J. Appl. Phys. **78** (1995) 5362.
23) E. Kobeda and E. A. Irene: J. Vac. Sci. Technol. B **7** (1989) 163.